Supplementary information

S1 Population density of the Po Valley

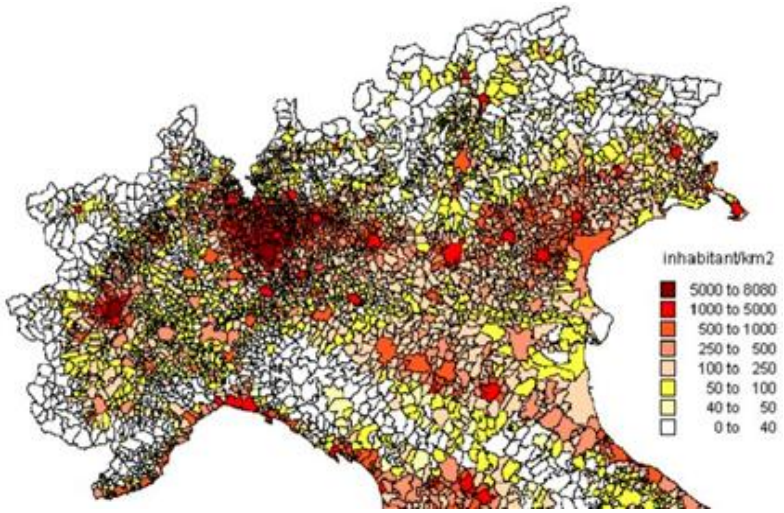

Figure S1. Population density of the Po Valley region. The most populated areas are Milan (north, north-west) and Turin (west). Source: Baklanov and Mahura, 2010.

S2 Emission sources of pollutants in the Po Valley

Table S2. Percentage of the different emission sources classified by macro-sectors (MS) for the Po Valley, 2013. Source: Raffaelli et al. (2020).

Macro-sectors	NH_3	Non-Methane Organic Compound (NMVOC)	NMVOC without MS10and MS11	NOx	PM_{10}	SO_2
MS1—Combustion in energy and transformation industries	0%	0%	0%	6%	1%	18%
MS2—Non-industrial combustion plants	0%	5%	11%	9%	56%	7%
MS3—Combustion in manufacturing industry	0%	1%	2%	15%	4%	41%
MS4—Production processes	0%	4%	9%	3%	3%	21%
MS5—Extraction and distribution of fossil fuel and geothermal energy	0%	2%	4%	0%	0%	0%
MS6—Solvent and other product	0%	28%	58%	0%	5%	0%
MS7—Road transport	1%	6%	14%	50%	20%	1%
MS8—Other mobile sources and machinery	0%	1%	2%	13%	4%	10%
MS9—Waste treatment and disposal	1%	0%	0%	1%	0%	2%
MS10—Agriculture	97%	22%	0%	1%	4%	0%
M11—Other sources and sinks	0%	31%	0%	0%	3%	0%
Total Emissions	100%	100%	100%	100%	100%	100%

S3 International studies investigating pollution pathways over the Po Valley

- The TRANSALP project was carried out as part of EUROTRAC/TRACT 1989-1991 (European Experiment on Transport and Transformation of Environmentally Relevant Trace Constituents in the Troposphere over Europe/ Transport of Air Pollutants over Complex Terrain). It comprised three tracer field experiments (1989, 1990, and 1991) performed in the south of Switzerland to evaluate the meso-scale transport and diffusion of pollutants across the Alps. The experiments studied the complex mountain topography, focusing on the mountain-plain circulation system and the meteorological conditions that favour the exchange of transalpine air masses and proved the occurrence of transport in the south-north direction (Ambrosetti et al., 1998).

- PIPAPO (Pianura Padana Produzione di Ozono) campaign (May-June 1998) was part of the EUROTRAC-2 LOOP (Limitation Of Oxidant Production) subproject and combined airborne and ground-based measurements with chemical transport models to analyse VOC/NO_x sensitivity of O_3 production in the Milan plume and pollutants dispersion in the surrounding region. The results of PIPAPO showed the recirculation of polluted air masses in the emission area of Milan, after their injection in the mountain valleys. No evidence of transalpine flow of pollution was found during the project. However, as this study specifically targeted the surroundings of Milan and not the neighbouring regions and was restricted to the late spring months of May and June, it cannot be considered representative for the PP dispersion of pollutants (Neftel et al., 2002; Dosio et al., 2002).
- EU FP7 projects MEGAPOLI and CityZen included the PP among the investigated major population centres (MPCs). The two projects took place in the period 2008-2011 to assess the effect of MPC emissions on a larger scale and investigate the exchange with the neighbouring regions (Baklanov, 2011; Gauss, 2011). MEGAPOLI showed that under anti-cyclonic conditions, the PP footprint extends to southern Europe and northern Italy, while larger urban agglomerates like Milan are responsible for high levels of $PM_{2.5}$ inside the region (Baklanov, 2011).
- The APPRAISAL survey (2011-2014) was a further instrument of the EU FP7 to investigate air quality management in Europe. A section of the project dealt with the PP region Emilia-Romagna and listed the abatement strategies for NH_3, NO_x and PM_{10} (Belis et al., 2017).
- In 2017, EU LIFE-IP Clean Air PREPAIR (Po Regions Engaged to Policies of Air; https://www.lifeprepair.eu/) started after the stipulation of an agreement between the governments of Italy and Slovenia, the administrative PP regions, and their environmental organisations. Slovenia was involved in the project in order to extend the air pollution management to the Adriatic Sea area. The objectives of LIFE-IP-PREPAIR are the reduction of pollution levels in the PP through the implementation of abatement strategies and the evaluation of their effectiveness. Another aim of the project is to raise the environmental awareness in the community and create a network at the national and regional level between researchers, political and socio-economical entities. The project is due to end in 2024 (Raffaelli et al., 2020).
- RI-URBANS (2021-2025, https://riurbans.eu) is a H2020 Green Deal Project that integrates European air quality monitoring networks with research infrastructures (RI), e.g., ACTRIS, ICOS, IAGOS, to enhance real-time observations of atmospheric pollutants, including aerosols. The Po Valley is a key pilot area where advanced monitoring techniques are tested to assess air pollution exposure, with specific activities in Milan and Bologna focusing on black carbon, particulate matter composition, and urban pollution sources (Apituley et al., 2024).
- TEAMx (Rotach et al, 2022; https://www.teamx-programme.org/) investigates atmospheric exchange processes over mountainous regions, with some observational campaigns extending to areas near the Po Valley. Using ground-based, remote sensing, and aircraft measurements, the initiative helps improve the understanding of boundary layer dynamics and transport processes, which influence aerosol distribution and air quality in the surrounding regions.
- MAIA (Diner et al; 2018; https://maia.jpl.nasa.gov) is a partnership between NASA and the Italian Space Agency (Agenzia Spaziale Italiana or ASI) aimed at studying the health effects of airborne particulate matter. It combines surface-based air monitoring data and satellite observations to analyze aerosol composition, pollution variability, and in turn potential health impacts. To support ASI research goals, three MAIA primary

target areas have been established in Italy. These cover a number of cities including main urban centers in the Po valley such as Milan, Turin, and Bologna.

S4 Tracks of E-EU-03 and E-EU-06

Table S4. Approximate time and location of altitude changes as indicated in Fig.S3: a) E-EU-03, and b) E-EU-06. Altitudes are given in m above sea level (a.s.l.)

a)

waypoints	date and time (UTC)	(lat. °N, long. °E)	altitude a.s.l. (m)
3a	11.07.2017 10:34	(45.7, 11)	5430
3b	11.07.2017 10:39	(45.6, 10.6)	3530
3c	11.07.2017 10:49	(45.6, 9.6)	3530
3d	11.07.2017 10:51	(45.6, 9.5)	2900
3e	11.07.2017 15:26	(45.6, 11.7)	1010
3f	11.07.2017 15:31	(45.5, 11.8)	3220
3g	11.07.2017 15:39	(45.4, 12.6)	3220

b)

waypoints	date and time (UTC)	(lat. °N, long. °E)	altitude a.s.l. (m)
6	2017-07-20 09:42	(45.5, 13.4)	3200
6a	2017-07-20 09:49	(44.9, 13.5)	3200
6b	2017-07-20 09:53	(45.1, 13.5)	1630
6c	2017-07-20 09:59	(45.5, 13.4)	1630
6d	2017-07-20 10:02	(45.3, 13.4)	520
6e	2017-07-20 10:10	(44.9, 13.4)	520
6f	2017-07-20 10:21	(44.8, 12.6)	520
6g	2017-7-20 10:37	(45.7, 13.2)	520
6h	2017-7-20 10:39	(45.6, 13.1)	1600
6i	2017-7-20 10:54	(44.8, 12.5)	1600
6j	2017-7-20 10:58	(44.9, 12.6)	3220
6k	2017-7-20 11:10	(45.7, 13.2)	3220
6l	2017-7-20 11:19	(45.3, 12.8)	840
6m	2017-7-20 12:07	(44.9, 9)	840
6n	2017-7-20 12:11	(44.6, 9)	2590
6o	2017-7-20 12:19	(44.1, 9)	2590

S5 Distribution of emissions in the PP

The ARPAs (Environmental Protection Regional Agencies) monitor the air quality in the Italian regions by measuring air composition through ground-based stations. In 2017 and 2015, the software INEMAR (INventario EMissioni ARia, https://www.inemar.eu/) and IREA (Inventario Regionale delle Emissioni in Atmosfera, https://servizi.regione.piemonte.it/catalogo/inventario-regionale-delle-emissioni-atmosfera-irea) were used to estimate annual emissions of the main macropollutants (CO_2, CO, CH_4, NO_x, N_2O, NH_3, SO_2, VOCs, $PM_{2.5}$, and PM_{10}) from anthropogenic and biogenic sources in the PP regions. The emission sources are divided into 11 groups or macro-sectors based on the international classification EMEP (Co-operative Programme for Monitoring and Evaluation of Long RangeTransmission of Air Pollution in Europe) – CORINAIR (CoORdination of Information on the Environment AIR emission)/SNAP (Selected Nomenclature for sources of Air Pollution). The total annual emissions (see Fig. S5.1) show that the provinces of Milan, Turin and Venice and the south of Lombardy are the main polluted areas. Figure S5.2 indicates the groups of emissions divided by region, showing that Lombardy is the most polluted region with main emitting groups G1 (Combustion in energy and transformation industry), G2 (Non-industrial combustion processes), G3 (Combustion in manufacturing industry), and G7 (Road transport).

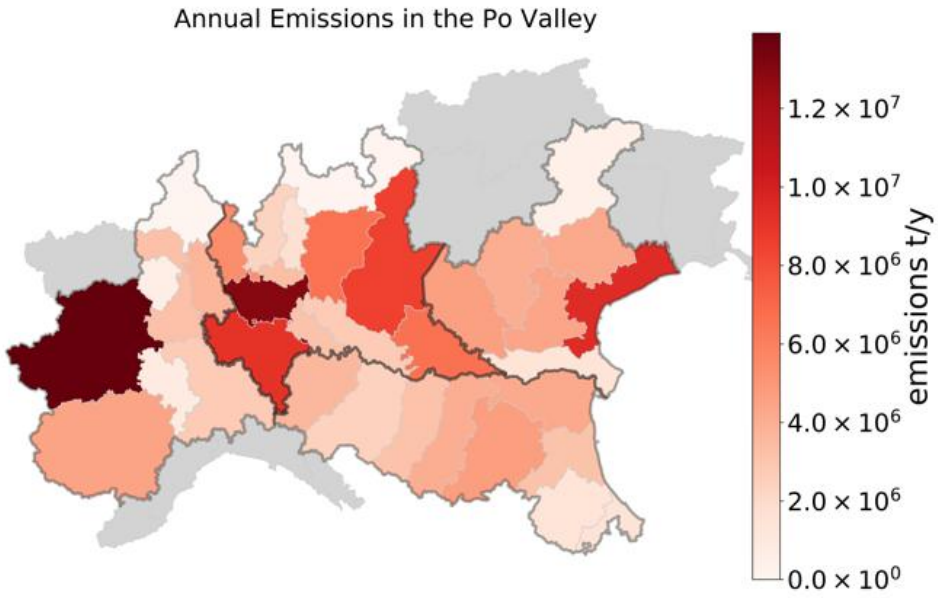

Figure S5.1. Emissions per province according to the EMEP-CORINAIR/SNAP classification. Data sources: IREA 2015, INEMAR 2017.

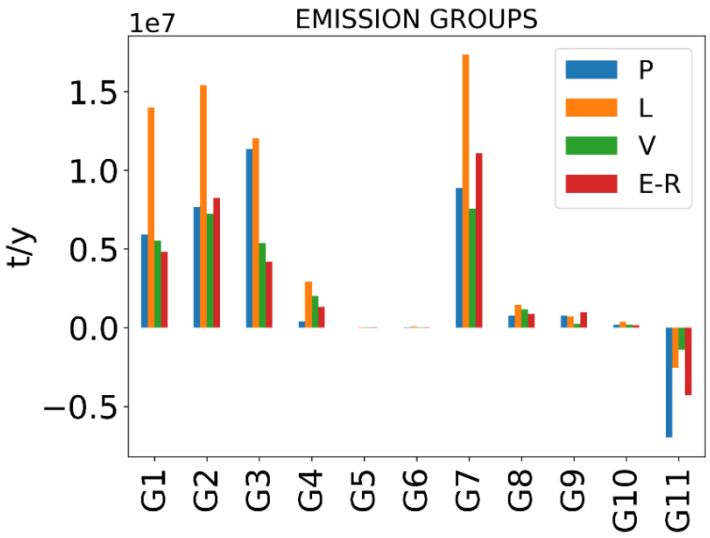

Figure S5.2. Emissions per region divided into groups of emission according to the EMEP-CORINAIR/SNAP classification. P is Piedmont, L is Lombardy, V is Veneto and E-R is Emilia-Romagna. Groups are: G1: Combustion in energy and transformation industry; G2: Non-industrial combustion processes; G3: Combustion in manufacturing industry; G4: Production processes; G5: Extraction and distribution of fossil fuels and geothermal energy; G6: Solvent and other product use; G7: Road transport; G8: Other mobile sources and machinery; G9: Waste treatment and disposal; G10: Agriculture; G11: Other sources and sinks. Data sources: IREA 2015, INEMAR 2017.

S6 Ground-based stations of the ARPA air quality-monitoring system (AQMN)

Table S6.1. Ground-based stations selected along the flight track of the HALO flights. T: temperature, P: pressure, RH: relative humidity, ws: wind speed; wd: wind direction. Data source: ARPAs' dataset.

station number	station name	station type	measurements	time resolution	(lat. °N, lon. °E)
1	Novi Ligure-Gobetti	Urban traffic	NO, NO_2, NO_x, PM_{10}, ws, wd	Hourly (daily for PM)	(44.76, 8.8)
2	Voghera Pozzoni	Urban background	NO_2, NO_x, O_3, CO, C_6H_6, PM_{10}, ws, wd	Hourly (daily for PM)	(45.0, 9.01)
3	S. Rocco al Porto	Suburban background	NO_2, NO_x, CO, PM_{10}	Hourly (daily for PM)	(45.08, 9.7)
4	Cremona Fatebenefratelli	Urban background	NO_2, NO_x, NH_3, O_3, CO, SO_2, ws, wd	1 hour	(45.14, 10.04)
5	Viadana	Urban background	NO_2, NO_x, O_3	Hourly	(44.92, 10.52)
6	Mantova Gramsci	Urban traffic	NO_2, NO_x, CO, C_6H_6, SO_2, PM_{10}, ws, wd	Hourly (daily for PM)	(45.15, 10.78)
7	Rovigo Centro	Urban traffic	NO_2, O_3, CO, C_6H_6, SO_2, PM_{10}, ws, wd	Hourly (daily for PM)	(45.07, 11.78)
8	Bra- Madonna Fiori	Urban traffic	NO, NO_2, NO_x, PM_{10}, ws, wd	Hourly (daily for PM)	(44.71, 7.84)
9	Vinchio- San Michele	Rural background	NO, NO_2, NO_x, O_3, PM_{10}, $PM_{2.5}$, ws, wd	Hourly (daily for PM)	(44.8, 8.31)
10	Baldissero-Torinese	Rural background	NO, NO_2, NO_x, O_3, CO, ws, wd	Hourly	(45.06, 7.8)

11	Novara- Verdi	Urban background	NO, NO_2, NO_x, O_3, PM_{10}, $PM_{2.5}$, ws, wd	Hourly (daily for PM)	(45.44, 8.62)
12	Saronno Santuario	Urban background	NO_2, NO_x, O_3, PM_{10}, ws, wd	Hourly (daily for PM)	(45.63, 9.04)
13	Sesto San Giovanni	Urban traffic	NO_2, NO_x, CO, $PM_{2.5}$, ws, wd	Hourly (daily for PM)	(45.53, 9.24)
14	Osio Sotto	Suburban background	NO_2, NO_x, O_3, PM_{10}, ws, wd	Hourly (daily for PM)	(45.62, 9.61)
15	Sarezzo	Urban background	NO_2, NO_x, O_3, CO, PM_{10}, ws, wd	Hourly (daily for PM)	(45.65, 10.21)
16	Brescia Via Turati	Urban traffic	NO_2, NO_x, CO, C_6H_6, ws, wd	Hourly	(45.54, 10.23)
17	San Felice	Urban traffic	NO_2, CO, SO_2	Hourly	(45.55, 11.53)
18	Bassano	Urban background	NO_2, O_3, $PM_{2.5}$, ws, wd	Hourly (daily for PM)	(45.76, 11.74)
19	Padova Arcella	Urban traffic	NO_2, CO, PM_{10}, ws, wd	Hourly (daily for PM)	(45.43, 11.89)
20	Genoa_Genova - Quarto	Urban background	NO, NO_2, O_3, SO_2	Hourly	(44.39, 8.99)
21	Genoa_Genova – Corso Firenze	Urban background	NO, NO_2, O_3, CO, SO_2	Hourly	(44.42, 8.93)
22	Genoa_Genova – Via Buozzi	Urban traffic	NO, NO_2, CO, SO_2	Hourly	(44.41, 8.91)
23	Ispra	Rural background	NO, NO_2, O_3, CO, SO_2, PM_{10}, ws, wd, air T, RH, air P, solar radiation	10-minutes	(45.807, 8.631)

Table S6.2.Ground-based trace gas instrumentation of the ARPA AQMN stations

Species	**Technique/ Instrument**
NO, NO_2, NO_x	Chemiluminescence
CO	Spectrophotometry IR
SO_2	Molecular Fluorescence Spectroscopy
O_3	UV-photometry

S7 LiDAR instruments

Vertical profiles from the following LiDAR systems were considered in this work:

- Automated Lidar-Ceilometer (ALC) located at the University Milano Bicocca as part of the Italian ALICENET network. It is an OTT_HydroMet (former Lufft) CHM15k-Nimbus working at a single wavelength of 1064 nm, with a 15 s temporal resolution and 15 m vertical resolution. Detailed information on the ALICENET network and data processing are given in Bellini et al. (2024)
- UV LIDAR in San Pietro Capofiume, operated by the University of Naples Federico II (Boselli et al, 2021). It was working at a wavelength of 355 nm, with depolarisation capabilities. The particle backscatter coefficient β_p and particle linear depolarization ratio δ_p profiles were retrieved using the Klett inversion (Klett, 1981). The first valid measurement is at 270 m due to the incomplete overlap between the laser and the field of view of the telescope closer to the surface (Wandinger, 2005).
- LIDAR of the JRC in Ispra, which operates at three different wavelengths: 1064 nm, 532 nm and 355 nm. The βp and the δ_p profiles of the lidar in Ispra have been retrieved using the ACTRIS-EARLINET (Aerosol, Clouds and Trace Gases Research Infrastructure-European Aerosol Research Lidar Network) Single Calculus Chain (https://www.earlinet.org).

S8 Average mixing ratios and ratios between species measured during E-EU-06 over the Po Plain

Table S8: Mean (mean), standard deviation (std) and quartiles (25th, 50th, 75th) concentrations of a) selected measured trace gases, b) aerosol particles, and c) ratios between selected trace gases for the E-EU-06 flight over the Po Plain: Note that HCHO and NO_2 were remotely measured by the mini DOAS instrument. BC, NO_3^-, SO_4^{2-} are given for standard temperature and pressure conditions. The periods within the BL are marked in yellow.

a)

flight legs		6b-6c	6d-6e	6e-6f	6f-6g	6h-6i	6j-6k	6l-to CPP	CPP	CPP/GG	6l-6m	6n-6o
time		09:52-10:00	10:02-10:10	10:10-10:20	10:21-10:37	10:39-10:54	10:57-11:10	11:19-11:30	11:30-11:50	11:50-12:07	11:19-12:06	12:10-12:19
altitude (m)	mean	1626	516	522	519	1631	3229	839	838	833	836	2579
	std	2	1	3	4	6	2	1	3	2	4	47
CO (ppb)	mean	135	126	131	122	109	79	127	117	118	120	80
	std	3	4	10	7	15	1	6	8	6	8	2
	25th	134	123	122	116	92	78	122	111	114	114	79
	50th	135	125	135	123	111	79	125	116	119	120	80
	75th	137	129	137	126	121	80	133	124	124	126	82
SO_2 (ppt)	mean	669	1895	1094	978	269	143	908	735	1318	991	116
	std	80	1025	391	327	158	21	131	239	642	512	19
	25th	611	1342	959	687	169	131	807	583	751	640	104
	50th	664	1671	1068	979	193	145	906	691	1198	827	115
	75th	723	2090	1224	1197	318	157	995	825	1792	1143	128
NO (ppb)	mean	0.20	0.27	0.27	0.21	0.16	0.09	0.24	0.41	0.74	0.49	0.04
	std	0.08	0.07	0.12	0.09	0.03	0.03	0.06	0.16	0.31	0.29	0.01
	25th	0.13	0.25	0.18	0.17	0.14	0.07	0.20	0.30	0.48	0.28	0.04
	50th	0.20	0.28	0.26	0.20	0.16	0.07	0.22	0.43	0.62	0.45	0.05
	75th	0.26	0.32	0.33	0.22	0.18	0.13	0.29	0.50	1.00	0.58	0.05
NO_2 (ppt)	mean	204	378	472	426	136	98	517	982	1360	1014	131
	std	11	49	45	53	30	10	84	285	487	468	14
	25th	200	335	438	390	106	92	449	768	977	655	122
	50th	206	360	470	421	137	96	478	891	1365	875	130
	75th	210	430	501	469	165	102	574	1106	1769	1329	138
NO_y (ppb)	mean	7.2	3.0	6	4.1	3.5	0.9	5	7	8	7	1.1
	std	0.4	0.7	1	0.9	2	0.1	1	2	3	3	0.2
	25th	6.9	2.6	5	3.3	2	0.9	4	5	6	5	1.0
	50th	7.1	2.8	6	3.7	4	0.9	5	6	8	6	1.1
	75th	7.3	3.2	7	4.7	5	1.0	6	7	11	9	1.2
RO_2 (ppt)	mean	88	86	103	90	84	64	76	51	62	61	45
	std	8	8	11	10	20	3	10	11	22	18	13
	25th	81	81	97	86	70	62	70	44	50	49	38
	50th	89	85	100	92	81	62	76	51	63	58	44
	75th	95	91	108	97	93	64	82	57	81	74	48
HCHO (ppt)	mean	1299	1639	1919	1613	1046	541	1463	1680	2173	1806	544
	std	51	93	118	204	151	38	99	111	264	337	35
	25th	1256	1571	1844	1415	876	509	1391	1593	2037	1563	520
	50th	1325	1610	1932	1558	1117	550	1404	1685	2166	1722	533
	75th	1336	1732	1991	1801	1163	561	1556	1763	2274	2048	574
C_3H_6O (ppt)	mean	3205	2626	3437	2752	2332	1703	3319	2926	2855	3002	1726
	std	189	78	367	307	379	94	199	380	281	354	60
	25th	3030	2576	3396	2574	2016	1668	3163	2678	2747	2788	1703
	50th	3292	2580	3503	2640	2122	1721	3297	2863	2907	3053	1723
	75th	3321	2709	3564	2946	2724	1756	3472	3258	3056	3260	1757
O_3 (ppb)	mean	91	75	79	74	67	51	78	72	69	72	55
	std	4	3	5	3	13	1	4	3	5	5	2
	25th	89	73	74	72	54	51	75	70	64	69	54
	50th	92	74	81	74	69	51	77	72	70	73	55
	75th	93	77	83	75	77	52	81	73	74	75	56

b)

flight legs		6b-6c	6d-6e	6e-6f	6f-6g	6h-6i	6j-6k	6l-to CPP	CPP	CPP/GG	6l-6m	6n-6o
time		09:529-10:00	10:02-10:10	10:10-10:20	10:21-10:37	10:39-10:54	10:57-11:10	11:19-11:30	11:30-11:50	11:50-12:07	11:19-12:06	12:10-12:19
altitude (m)	**mean**	**1626**	**516**	**522**	**519**	**1631**	**3229**	**839**	**838**	**833**	**836**	**2579**
	std	2	1	3	4	6	2	1	3	2	4	47
NO_3^- (μgm^{-3})	**mean**	**5.4**	**0.21**	**2**	**0.3**	**1.46**	**0.06**	**1.2**	**2**	**1.4**	**2**	**0.06**
	std	0.6	0.08	1	0.4	1.48	0.02	0.7	1	1.0	1	0.02
	25th	5.0	0.15	1	0.1	0.09	0.05	0.6	1	0.3	1	0.05
	50th	5.4	0.16	2	0.2	1.07	0.06	1.1	1	1.6	1	0.06
	75th	5.6	0.27	3	0.2	2.35	0.07	1.7	3	2.1	2	0.07
SO_4^{2-}(μgm^{-3})	**mean**	**2.0**	**2.2**	**1.9**	**2**	**1.27**	**0.62**	**2.3**	**1.4**	**1.6**	**1.7**	**0.64**
	std	0.1	0.4	0.3	1	0.49	0.05	0.2	0.1	0.2	0.4	0.09
	25th	2.0	2.0	1.8	2	0.80	0.57	2.2	1.3	1.5	1.4	0.60
	50th	2.0	2.2	1.9	2	1.23	0.61	2.3	1.4	1.6	1.5	0.65
	75th	2.1	2.4	2.0	3	1.58	0.64	2.4	1.5	1.7	1.9	0.68
BC (μgm^{-3})	**mean**	**0.4**	**0.4**	**0.4**	**0.4**	**0.21**	**0.09**	**0.4**	**0.4**	**0.4**	**0.4**	**0.08**
	std	0.1	0.1	0.1	0.1	0.13	0.06	0.1	0.1	0.1	0.1	0.05
	25th	0.3	0.3	0.4	0.3	0.09	0.06	0.3	0.3	0.3	0.3	0.05
	50th	0.4	0.4	0.4	0.4	0.21	0.07	0.4	0.4	0.4	0.4	0.07
	75th	0.4	0.4	0.5	0.4	0.30	0.10	0.5	0.5	0.5	0.5	0.09

c)

flight legs		6b-6c	6d-6e	6e-6f	6f-6g	6h-6i	6j-6k	6l-to CPP	CPP	CPP/GG	6l-6m	6n-6o
time		09:53-10:00	10:02-10:10	10:10-10:20	10:21-10:37	10:39-10:54	10:57-11:10	11:19-11:30	11:30-11:50	11:50-12:07	11:19-12:06	12:10-12:19
altitude (m)	**mean**	**1626**	**516**	**522**	**519**	**1631**	**3229**	**839**	**838**	**833**	**836**	**2579**
	std	2	1	3	4	6	2	1	3	2	4	47
NO_y/CO	**mean**	0.053	0.024	0.044	0.033	0.030	0.012	0.037	0.055	0.070	0.057	0.014
	std	0.003	0.005	0.007	0.007	0.010	0.002	0.009	0.017	0.025	0.023	0.002
	25th	0.052	0.021	0.038	0.027	0.018	0.011	0.028	0.042	0.048	0.039	0.013
	50th	0.053	0.022	0.046	0.032	0.033	0.011	0.038	0.052	0.068	0.051	0.014
	75th	0.054	0.026	0.049	0.038	0.038	0.013	0.045	0.062	0.086	0.072	0.015
NO_y/NO_2	**mean**	35	8.1	12	9	24	10	9	7	6	7	9
	std	3	1.0	2	1	7	2	2	2	1	2	1
	25th	33	7.4	10	8	17	9	8	5	5	6	8
	50th	35	8.1	13	9	25	10	8	7	6	7	8
	75th	37	8.6	14	10	28	11	10	8	7	8	9
HCHO/CO	**mean**	0.010	0.013	0.015	0.013	0.010	0.007	0.012	0.015	0.018	0.015	0.007
	std	0.000	0.001	0.001	0.002	0.001	0.001	0.001	0.001	0.002	0.003	0.000
	25th	0.009	0.012	0.014	0.012	0.009	0.006	0.011	0.014	0.017	0.013	0.006
	50th	0.010	0.013	0.015	0.013	0.010	0.007	0.012	0.015	0.018	0.015	0.007
	75th	0.010	0.014	0.015	0.014	0.010	0.007	0.012	0.015	0.019	0.018	0.007
CO/BC	**mean**	314	351	312	346	625	710	308	310	325	315	898
	std	18	46	52	46	270	63	61	43	62	55	137
	25th	305	309	299	317	390	680	270	278	274	271	809
	50th	309	348	304	344	510	690	276	309	321	311	898
	75th	318	396	310	358	890	717	358	348	363	356	963

S9 COSMO wind simulation over the PP

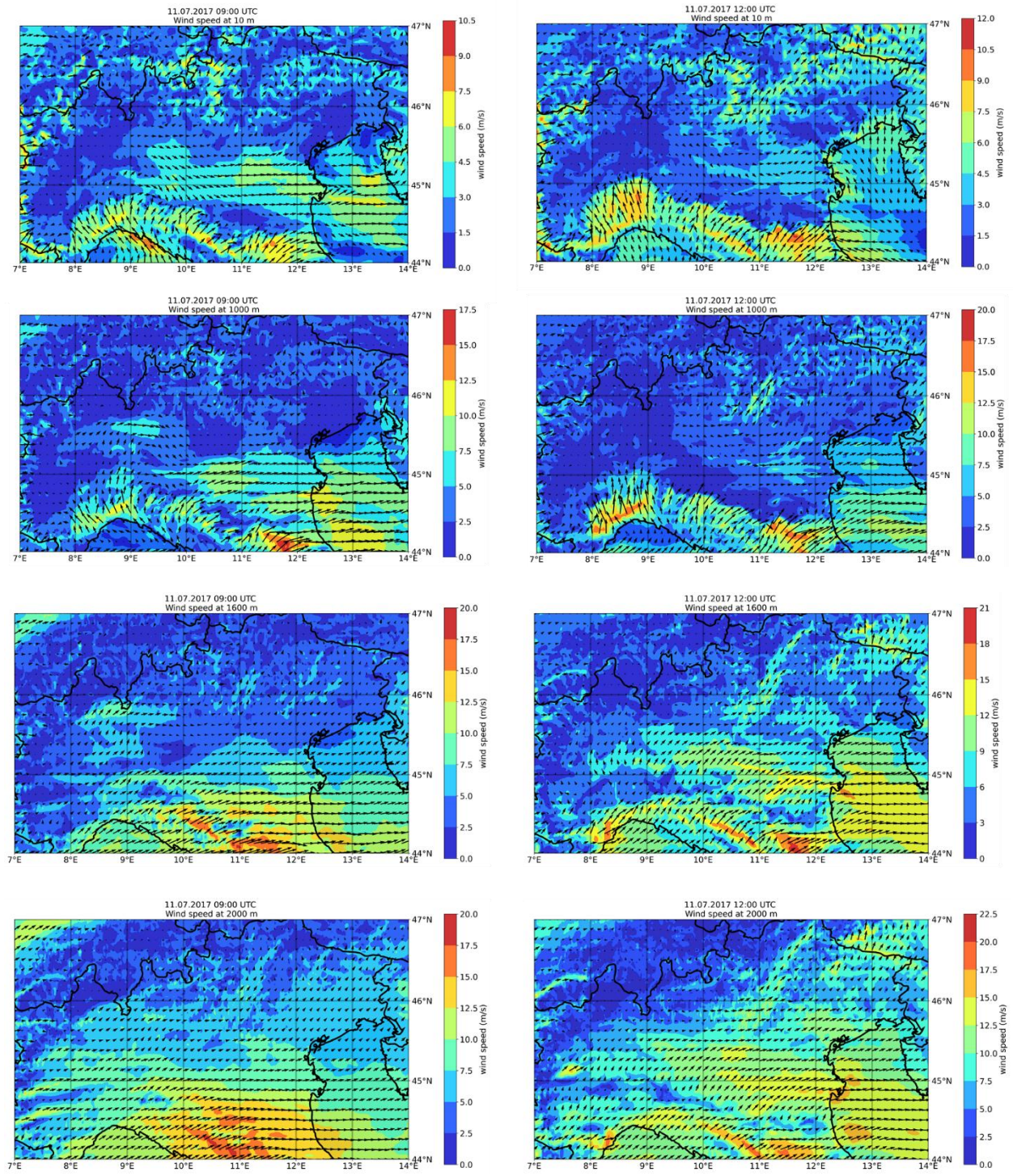

Figure S9.1. Wind simulation over the PP by COSMO on 11 July.2017 at 9 UTC (left) and 12 UTC (right) for 10 m, 1000 m, 1600 m, and 2000 m altitude a.s.l. Please note changes in the scale of the wind speed (ws).

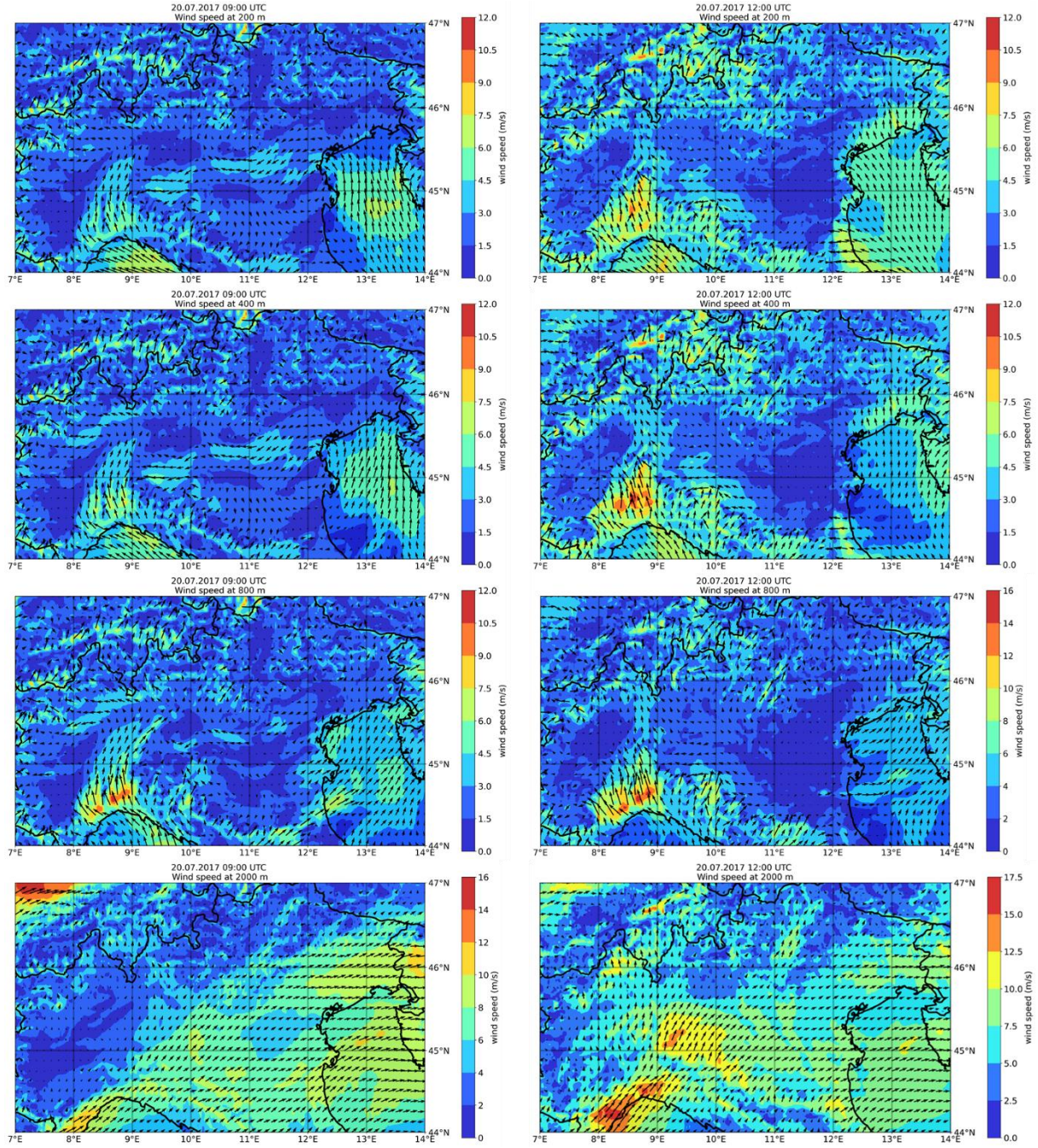

Figure S9.2. Wind simulation over the PP by COSMO on 20 July.2017 at 9 UTC (left) and 12 UTC (right) for 200 m, 400 m, 800 m, and 2000 m altitude a.s.l. Please note the changes in the scale of the wind speed.

S10 Sensitivity study of COSMO-LAGRANTO wind field

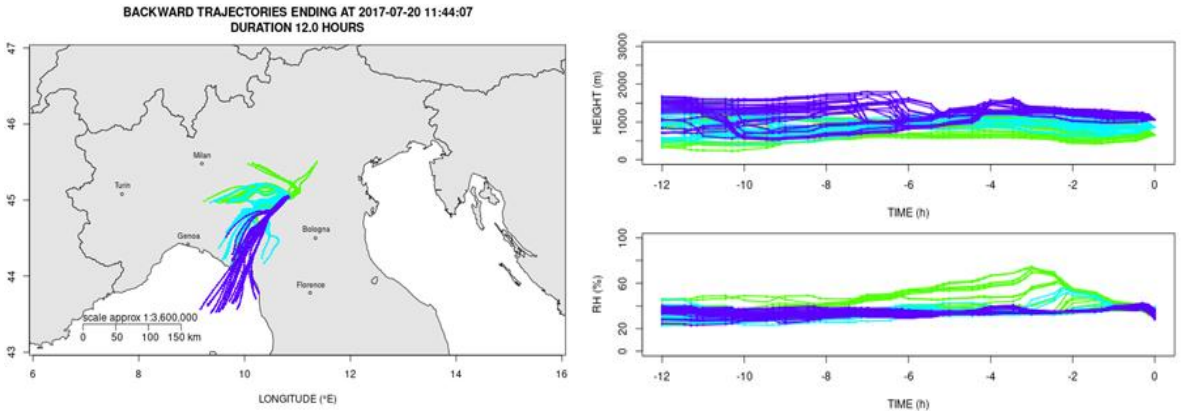

Figure S10. COSMO-LAGRANTO 12-hours back-trajectories from a selected point of the E-EU-06 flight track. Back-trajectories start inside a 2-km diameter circle at three different altitudes (green: HALO altitude – 200m, blue: HALO altitude of 840 m, purple: HALO altitude + 200m).

S11 Ratios between airborne and ground-based measurements

Table S11. Values of the ratios between airborne measurement during E-EU-06 and the stations of Vinchio and S.Rocco presented in Fig. 15 in the main text. The track from East to West over the PP comprises 10 points, each corresponding to 10 min averages.

#n of point	$NO_{2\ HALO}$ /$NO_{2Vinchio}$	$NO_{y\ HALO}$ /$NO_{xVinchio}$	$O_{3\ HALO}$ /$O_{3\ Vinchio}$	$CO_{\ HALO}$ /$CO_{S.Rocco}$
1	0.13	1.35	1.61	1.45
2	0.04	1.02	1.52	1.32
3	0.03	0.35	1.10	0.99
4	0.03	0.22	1.08	0.92
5	0.14	1.30	1.61	1.47
6	0.21	1.49	1.47	1.35
7	0.30	1.92	1.49	1.37
8	0.39	2.63	1.45	1.39
9	0.24	1.67	1.25	1.28
10	0.04	0.32	1.10	0.93

S12 Vertical profiles by Lidar & Ceilometers in the central PP area.

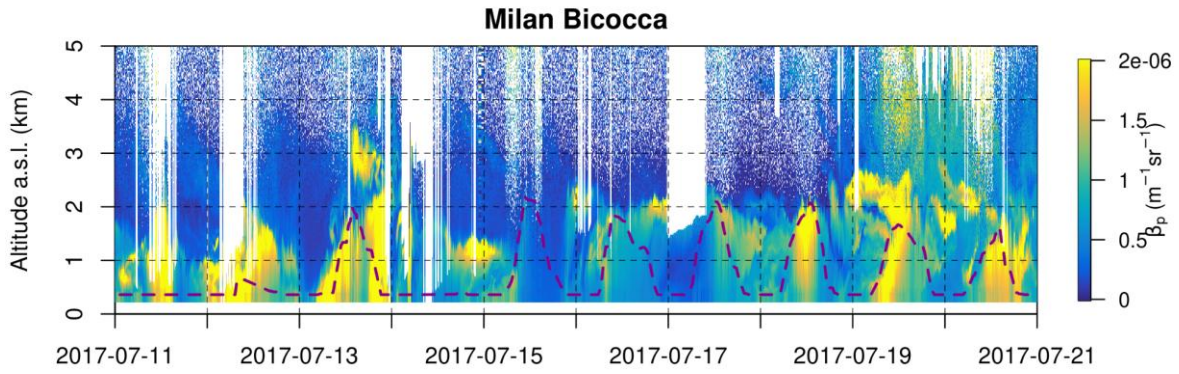

Figure S12.1: Continuous (0-24 UTC, x-axis) vertical profiles (0-5 km, y-axis) of aerosol backscatter at 1064 nm as observed by the ALICENET ALC system operating in Milan-Bicocca from July 11 to July 20, 2017. Cloud-affected profiles are filtered out from the cloud base upwards (white areas). The dashed line is the height of the Mixed Aerosol Layer (MAL) as derived from the Alicenet data processing (Bellini et al., 2024), it is artificially set to zero when persistence of clouds prevented the MAL retrieval.

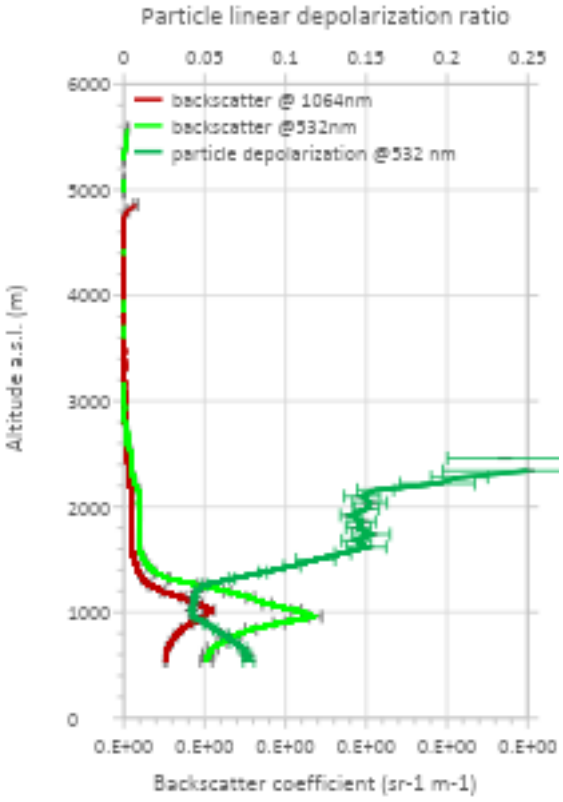

Figure S12.2 Vertical profiles of the particle light backscatter coefficient at 1064 and 532 nm, and the linear depolarization ratio at 532 nm measured by the LiDAR in Ispra on the 11 July at 10:17-10:42 h (UTC)

S13 Multi- Model Ensemble Desert Dust forecasts for the 20 July 2017

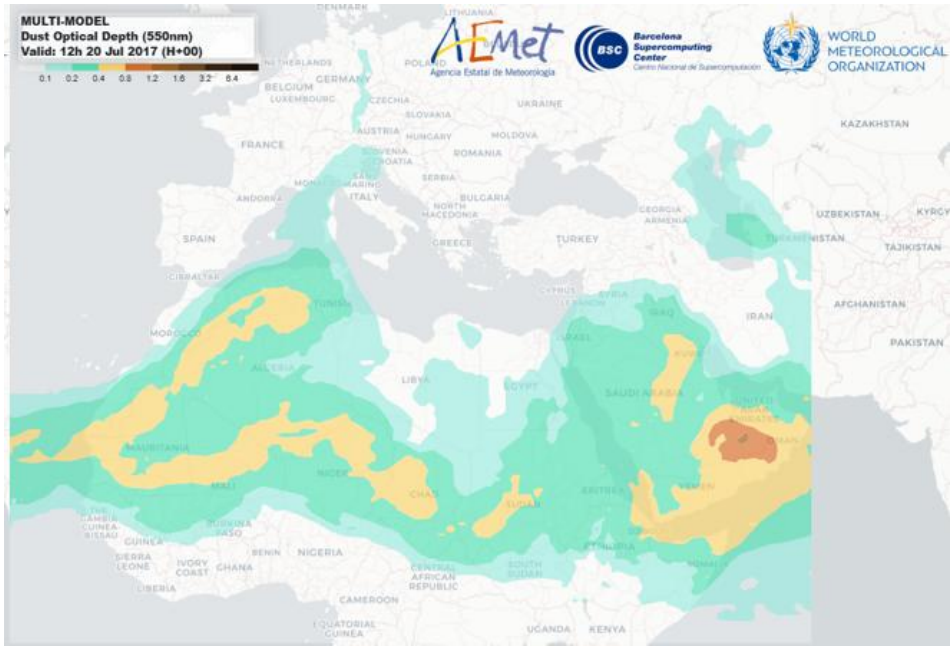

Figure S13: Dust Optical Depth at 550 nm derived from the Multimodel Ensemble at 12 UTC (i.e. approximately at the HALO overpass time) for July 20 2017, showing an optically thin desert dust layer advected over Northern Italy (credits: WMO Barcelona Dust Regional Center and the SDS-WAS)

References:

Apituley, A. et al.: Research Infrastructures Services Reinforcing Air Quality Monitoring Capacities in European Urban & Industrial AreaS (GA n. 101036245), https://riurbans.eu/wp-content/uploads/2024/04/RI-URBANS_D32_D4_11.pdf

Bellini, A., Diémoz, H., Di Liberto, L., Gobbi, G. P., Bracci, A., Pasqualini, F., and Barnaba, F.: ALICENET – an Italian network of automated lidar ceilometers for four-dimensional aerosol monitoring: infrastructure, data processing, and applications, Atmos. Meas. Tech., 17, 6119–6144, https://doi.org/10.5194/amt-17-6119-2024, 2024.

Boselli A. de Marco, C., Mocerino, L., Murena, F., Quaranta, F., Rizzuto, E., Sannino, A., Spinelli, N.,and Xuan, W.: Evaluating LIDAR Sensors for the Survey of Emissions from Ships at Harbor. In: Okada T., Suzuki K., Kawamura Y. (eds) Practical Design of Ships and Other Floating Structures. PRADS 2019. Lecture Notes in Civil Engineering, vol 64. Springer, Singapore. https://doi.org/10.1007/978-981-15-4672-3_49, 2021.

Diner, D.J., Boland, S.W., Brauer, M., Bruegge, C., Burke, K.A., Chipman, R., Di Girolamo, L., Garay, M.J., Hasheminassab, S., Hyer, E., Jerrett, M., Jovanovic, V., Kalashnikova, O.V., Liu, Y., Lyapustin, A.I., Martin, R.V., Nastan, A., Ostro, B.D., Ritz, B., Schwartz, J., Wang, J., Xu,, F.: Advances in multiangle satellite remote sensing of speciated airborne particulate matter and association with adverse health effects: from MISR to MAIA, J. Appl. Remote Sens. 12(4), 042603, doi: 10.1117/1.JRS.12.042603, 2018.

Rotach, M. W., Serafin, S., Ward, H. C., Arpagaus, M., Colfescu, I., Cuxart, J., De Wekker, S.F.J., Grubišic,V, Kalthoff, N., Karl, T., Kirshbaum, D.J., Lehner, M., Mobbs, S., Paci, A., Palazzi, E., Bailey, A., Schmidli, J., Wittmann, C., Wohlfahrt, G., and Zardi, D.: A Collaborative Effort to Better Understand, Measure, and Model Atmospheric Exchange Processes over Mountains. Bull. Amer. Meteor. Soc., 103, E1282–E1295, https://doi.org/10.1175/BAMS-D-21-0232.1, 2022.